

## Spin-waves in the mid-infrared spectrum of antiferromagnetic $\text{YBa}_2\text{Cu}_3\text{O}_{6.0}$

M. GRÜNINGER<sup>1</sup>, J. MÜNDEL<sup>1</sup>, A. GAYMANN<sup>1</sup>, A. ZIBOLD<sup>1</sup>  
H. P. GESERICH<sup>1</sup> and T. KOPP<sup>2</sup>

<sup>1</sup> *Institut für angewandte Physik, Universität Karlsruhe - D-76128 Karlsruhe, Germany*

<sup>2</sup> *Institut für Theorie der kondensierten Materie, Universität Karlsruhe  
D-76128 Karlsruhe, Germany*

(received 7 February 1996; accepted in final form 16 May 1996)

PACS. 74.72-h – High- $T_c$  cuprates.

PACS. 74.25Gz – Superconductivity: Optical properties.

PACS. 74.25Ha – Superconductivity: Magnetic properties.

**Abstract.** – The mid-infrared spin-wave spectrum of antiferromagnetic  $\text{YBa}_2\text{Cu}_3\text{O}_{6.0}$  was determined by infrared transmission and reflection measurements ( $\mathbf{k} \parallel c$ ) at  $T=10\text{K}$ . Excitation of single magnons of the optical branch was observed at  $E_{\text{op}} = 178.0\text{ meV}$ . Two further peaks at  $346\text{ meV}$  ( $\approx 1.94E_{\text{op}}$ ) and  $470\text{ meV}$  ( $\approx 2.6E_{\text{op}}$ ) both belong to the two-magnon spectrum. Linear spin-wave theory is in good agreement with the measured two-magnon spectrum, and allows to determine the exchange constant  $J$  to be about  $120\text{ meV}$ , whereas the intrabilayer coupling  $J_{12}$  is approximately  $0.5J$ .

High-temperature superconductors are basically layered copper-oxide materials. It is widely accepted that the relevant electronic degrees of freedom are confined to copper-oxide planes. The number of  $\text{CuO}_2$  planes per unit cell varies: *e.g.*,  $\text{La}_{2-x}\text{Sr}_x\text{CuO}_4$  exists in a single-plane form with a large spacing between planes of  $\approx 13.2\text{ Å}$ , and  $\text{YBa}_2\text{Cu}_3\text{O}_{6+x}$  has a double-layer structure with intra- and inter-bilayer spacings of  $\approx 3.3\text{ Å}$  and  $8.5\text{ Å}$ , respectively. Electronic correlations, and hence spin dynamics [1], may depend on the type of stacking of the planes. More specifically, a sizable coupling  $J_{12}$  between spins on adjacent planes of a bilayer will influence the spin excitation spectrum as well as the nature of the ground state. This may have been seen already in doped compounds: the normal-state spin susceptibility of  $\text{La}_{2-x}\text{Sr}_x\text{CuO}_4$  extrapolates to a finite value at zero temperature, whereas it extrapolates to zero for  $\text{YBa}_2\text{Cu}_3\text{O}_{6.6}$  [2]. This may be interpreted as a signature for the opening of a spin excitation gap in  $\text{YBa}_2\text{Cu}_3\text{O}_{6.6}$  at low temperatures <sup>(1)</sup> —a behaviour certainly not encountered in Fermi liquids. Further, a spin density wave ordering for  $\text{La}_{2-x}\text{Sr}_x\text{CuO}_4$  has been proposed, but for  $\text{YBa}_2\text{Cu}_3\text{O}_{6.6}$  a singlet pairing of spins in adjacent  $\text{CuO}_2$  planes with

---

<sup>(1)</sup> Other underdoped double- and triple-layer cuprates display a similar behaviour; for references see [1].

strong antiferromagnetic fluctuations within a plane [2]-[4]. Such a scenario seems to require an unrealistically large  $J_{12} \gtrsim 2.5J$  [5], where  $J$  is the in-plane exchange coupling of the Heisenberg Hamiltonian supposed to describe the low-energy spin dynamics of a single bilayer for zero doping ( $x = 0$ ). However, it was argued that, for finite doping, the itinerant carriers destroy the antiferromagnetism of the insulating phase and, therefore, much smaller values of  $J_{12}$  will produce a singlet interplane pairing in the conducting phase of  $\text{YBa}_2\text{Cu}_3\text{O}_{6.6}$ .

Up to now, no experimental evidence has been given of a sizable bilayer coupling ( $J_{12} \sim J$ ). In neutron scattering experiments on  $\text{YBa}_2\text{Cu}_3\text{O}_{6+x}$ , the in-plane coupling was determined from the dispersion of acoustic spin-waves and was found to be extremely large ( $J = 120 \pm 20$  meV [6],  $J = 150$  meV [7], both for  $x = 0.15$ ). Yet, no optical modes have been found for energies up to 60 meV [6], [8], suggesting a bilayer coupling of  $J_{12} \gtrsim 8$  meV. In Raman-scattering experiments on  $\text{YBa}_2\text{Cu}_3\text{O}_{6+x}$  a two-magnon peak was observed [9], [10].  $J$  was found to be consistent with the neutron scattering data, whereas  $J_{12}$  was neglected.

In this letter we report the first observation of an optical magnon peak and of the two-magnon spectrum in infrared spectroscopy of  $\text{YBa}_2\text{Cu}_3\text{O}_{6.0}$ . They allow to determine both  $J_{12}$  and  $J$ . Two resonances of the two-magnon spectrum confirm the location of the single magnon peak. Further, understanding the “antiferromagnetic limit”  $\text{YBa}_2\text{Cu}_3\text{O}_{6.0}$  will be crucial to interpret the excitations of carriers in doped  $\text{YBa}_2\text{Cu}_3\text{O}_{6+x}$  [11].

Due to the high resolution and the wide spectral range, optical spectroscopy is a powerful method to precisely determine energies of spin-waves. But, compared to other optical excitations such as infrared-active phonons, intraband and interband transitions, the absorption by magnons is two to three orders of magnitude weaker, yielding an optical conductivity of the order of 1 S/cm. Therefore, spin-wave excitations can be detected only in the transmittance spectra of thin single crystals. Up to now, investigations of this type have only been performed on single-layer cuprates [12]. Broad structures between 0.4 eV and 1.2 eV were observed which were interpreted as phonon-assisted multi-magnon processes [13].

The crystals with typical dimensions of  $1 \times 1 \times 0.1 \text{ mm}^3$  had been annealed in the UHV at 700 K for two days to exclude doping by excess oxygen. The samples are very close to the pure limit  $\text{YBa}_2\text{Cu}_3\text{O}_{6.0}$ , showing values of the conductivity function lower than 0.1 S/cm which is about three (five) orders of magnitude smaller than in  $\text{YBa}_2\text{Cu}_3\text{O}_{6.1}$  ( $\text{YBa}_2\text{Cu}_3\text{O}_7$ ) in the same spectral range. The measurements were performed using a Fourier-transform spectrometer Bruker IFS 113v in the spectral range between 85 meV and 1.5 eV. The samples were mounted on a diaphragm in a helium-flow cryostat. Reference spectra at each temperature were obtained using a second, identical diaphragm and a turning mechanism. Hence an absolute photometric accuracy of the transmission data of about 1% was achieved.

The conductivity function  $\sigma(\hbar\omega) = 2\omega\epsilon_0 n(\hbar\omega)k(\hbar\omega)$  can be calculated, if the sample thickness and both transmission and reflection spectra are known. Here,  $n$  and  $k$  denote the real and imaginary part of the refractive index. The sample thickness could be determined precisely from the spectral position of the interference maxima. Since reflection and transmission measurements use slightly different incident angles, and as furthermore the incident light beams are not completely parallel, there are still small interference structures in our plot of  $\sigma(\hbar\omega)$ .

Figure 1 displays reflectance and transmittance spectra, obtained at  $T = 10$  K on a single-crystalline platelet with a thickness of  $d = 125 \mu\text{m}$ . The resulting conductivity function is shown in fig. 3. Between 0.1 eV and 0.4 eV the measurements are dominated by interference effects, indicating regions of low absorption (as can be seen in  $\sigma$ ). Whereas the interference structure was precisely resolved by the spectrometer, it cannot be resolved in the figure.

The reflectance spectrum by itself is not sufficient to determine the excitations present in this spectral range, only the knowledge of both reflectance and transmittance provides full

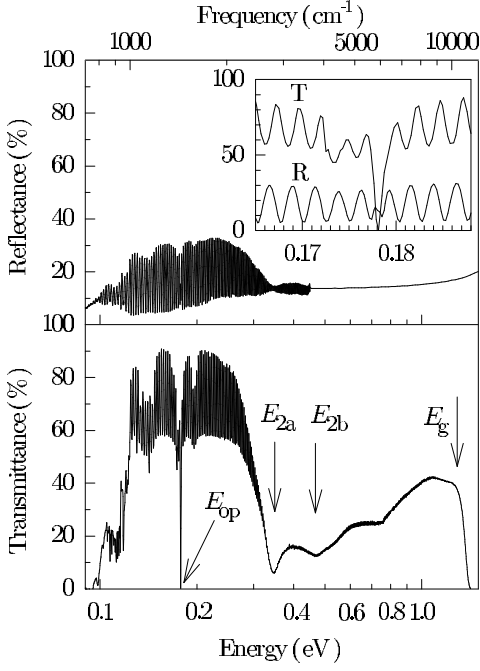


Fig. 1.

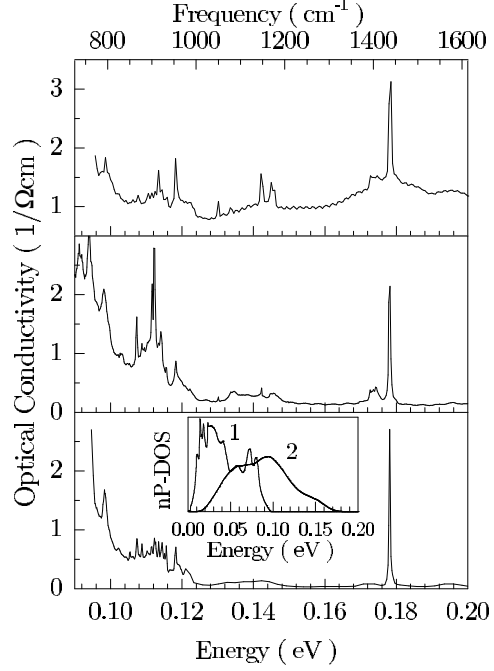


Fig. 2.

Fig. 1. – In-plane reflectance and transmittance spectra ( $\mathbf{k} \parallel c$ ) of a  $\text{YBa}_2\text{Cu}_3\text{O}_{6.0}$  single crystal with  $d=125\ \mu\text{m}$  at  $T=10\ \text{K}$ . The arrows mark absorption processes described in the text.

Fig. 2. – (Multi-) phonon and single-magnon spectrum for different samples of ultralow doped  $\text{YBa}_2\text{Cu}_3\text{O}_{6+x}$ . The lowest panel displays the (purest) sample of fig. 1 and 3 for comparison. The inset demonstrates that the two-phonon density of states (2P-DOS) vanishes close to  $E_{\text{op}}$ . The 2P-DOS (line 2) was calculated using experimental data for the phonon DOS (line 1) (see ref. [14]).

information. To discuss the different excitations a plot of  $\sigma(\hbar\omega)$  is most suitable. There, the exponentially decreasing high-energy tail of the highest fundamental phonon mode is observed up to 0.15 eV. Several smaller structures due to absorption by multi-phonons are superimposed on it. The main absorption features in the mid-infrared region are of magnonic origin. The excitation of single magnons of the optical branch is observed at  $E_{\text{op}} = 178.0\ \text{meV}$ . The oscillator strength of this magnon peak is approximately  $1.1 \cdot 10^{-4}\ \text{eV}^2$  <sup>(2)</sup>. A comparison of different crystals of  $\text{YBa}_2\text{Cu}_3\text{O}_{6+x}$  (fig. 2) shows that the multi-phonon spectrum differs from sample to sample due to a finite number of impurities whereas the optical magnon peak neither changes position nor shape. The sample of the upper panel is very weakly doped ( $x \ll 0.1$ ) and hence shows an increased conductivity.

The two peaks marked  $E_{2a}$  and  $E_{2b}$  both belong to the two-magnon spectrum, as will be discussed below. The broad high-energy tail of the spectrum is caused by higher multi-magnons. Finally, the steep increase of conductivity above 1.3 eV is due to the onset of intrinsic absorption, the excitation of carriers across the charge transfer gap.

In order to interpret this magnon spectrum, we use linear spin-wave (LSW) theory to

<sup>(2)</sup> Allowed processes involve a dipole transition to the oxygen  $p$ -orbitals and a spin-orbit interaction on the copper sites, which finally flips the spin. Summing over all processes, we find an oscillator strength close to the experimental value.

gain the excitation spectrum of localized spins on a bilayered square lattice. A Heisenberg Hamiltonian accounts for these low-energy excitations for zero doping:

$$H = J \sum_{a=1,2} \sum_{\langle i,j \rangle} \mathbf{S}_{a,i} \mathbf{S}_{a,j} + J_{12} \sum_i \mathbf{S}_{1,i} \mathbf{S}_{2,i}, \quad (1)$$

where  $i$  and  $j$  label nearest-neighbour sites in a two-dimensional square lattice and  $a \in \{1, 2\}$  labels the two different planes in a single bilayer. Each bond is counted once. Generally it is found that LSW supplies quantitatively satisfying results for the Néel ground state at low temperatures [15], [16], [1]. The (classical) Néel ground state  $\mathbf{S}_{1,i} = \pm(-1)^i S(1, 0, 0)$  is stabilized by a finite bilayer coupling  $J_{12}$  [17] ( $S = 1/2$ ). Spin-orbit effects are relatively small [17] and were neglected in eq. (1). However, the finite spin-orbit coupling is needed to couple the external electric field to a single magnon, and further to make two-magnon absorption possible for the considered crystal symmetry [18].

Due to the finite bilayer coupling, the classical one-magnon spectrum splits into acoustic and optical branches <sup>(3)</sup>:  $\hbar\omega_{\text{op/ac}}(\mathbf{k}) = SJ\sqrt{z^2 - \tau_{\mathbf{k}}^2 + 2(J_{12}/J) \cdot (z \pm \tau_{\mathbf{k}})}$ , where  $z = 4$  is the coordination number in a plane, and  $\tau_{\mathbf{k}} = 2(\cos(k_x a) + \cos(k_y a))$ .  $\mathbf{k}$  is within the magnetic Brillouin zone, and  $a$  is the lattice constant. Absorption experiments probe  $\mathbf{k} = 0$  with energy gap  $E_{\text{op}} \equiv \hbar\omega_{\text{op}}(\mathbf{k}=0) = 2(2S)\sqrt{J_{12}J}$  for the optical branch. The acoustic mode splits, due to the small spin-orbit coupling [17]. The gapped out-of-plane mode is indeed observed in neutron scattering experiments at  $E_{\text{ac}}(\mathbf{k}=0) \approx 4.5 \text{ meV}$  [8]. The splitting of the optical branch at  $\mathbf{k}=0$  may be estimated to be  $\Delta E_{\text{op}} \approx E_{\text{ac}}^2/2E_{\text{op}} \approx 1/18 \text{ meV}$ , a scale too small in comparison with the width of the optical magnon peak of about 1 meV to be resolved in our experiment<sup>(4)</sup>.

The two-magnon absorption is calculated with a coupling Hamiltonian of the form

$$H_1 = D \sum_{a,b} \sum_{\langle i,j \rangle} \mathbf{E} \cdot [(\mathbf{S}_{a,i} \times \mathbf{S}_{b,j}) \times \boldsymbol{\pi}_{a,i;b,j}], \quad (2)$$

where  $\boldsymbol{\pi}_{a,i;b,j}$  points in the direction of the vector joining the pair  $\langle a,i; b,j \rangle$  and  $\mathbf{E}$  is the electric-field vector [20]. This is the only coupling allowed by crystal symmetry for a nearest-neighbour two-magnon generation.  $D\boldsymbol{\pi}$  is found from a perturbation series in the nearest-neighbour exchange interaction and spin-orbit interaction [18]. Since we restrict ourselves to  $\mathbf{k} \parallel c$ , the two-magnon coupling is proportional to  $E^y \pi_{1,i;2,i}^z \cdot (S_{1,i}^- S_{2,i}^+ - S_{1,i}^+ S_{2,i}^-)$  which creates a singlet pair of magnons on adjacent planes. This type of magnon pair generation is a consequence of the spin alignment in the  $(x, y)$ -plane in the Néel ground state.

Absorption is not just determined by the convoluted density of states (DOS) of two magnons but also by the (local) interaction between the two magnons [20]. Therefore, absorption is not just characterized by a step-like increase at the optical two-magnon edge,  $2E_{\text{op}}$ , and a diverging DOS at the upper band edge (as for  $J_{12} = 0$ ). Rather, the local interaction will reduce the frustration produced by the two spin-flips and allow two optical magnons to form a nearly bound state below  $2E_{\text{op}}$ . Due to the admixture of acoustic magnons the bound state shows up as a resonance. A second broader resonance close to the band edge replaces the diverging two-magnon DOS for  $J_{12} > 0$ , similar to the well-known two-magnon peak in  $B_{1g}$  Raman scattering. Quantum fluctuations certainly broaden the two-magnon peaks.

The exact positions of both peaks depend upon the ratio  $J_{12}/J$ , as is displayed in the inset of fig. 3. For comparison with the experiment we introduced an additional decay rate for the two-magnon excited state of about  $0.09E_{\text{op}}$  to gain an optimal fit. Due to this additional broadening we obtain a value of approximately 0.58 for  $J_{12}/J$ , slightly higher than marked

<sup>(3)</sup>  $J_{12} = 2J_{12, \text{Bonesteel}}$  of ref. [17], eqs. (5.16) ff.

<sup>(4)</sup> The 1-magnon spectrum is discussed and portrayed, *e.g.*, in ref. [7] and in [19].

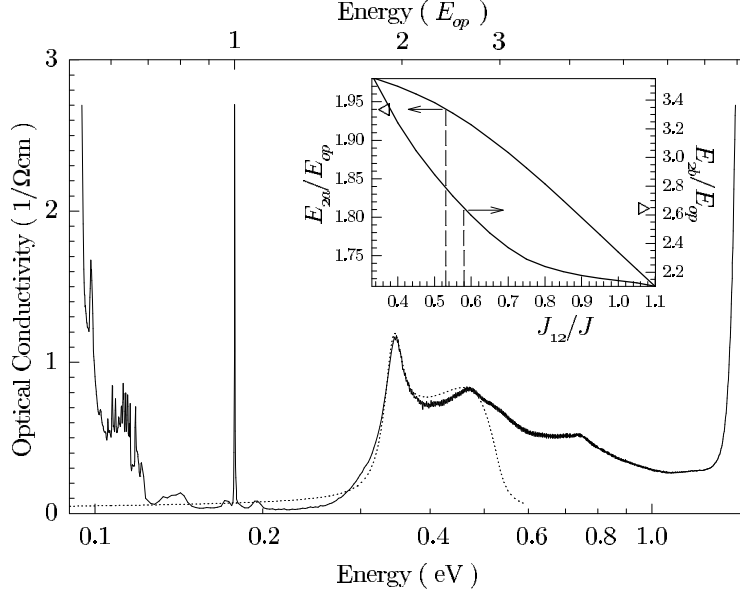


Fig. 3. – Solid line: optical conductivity for  $\mathbf{k} \parallel c$ , calculated from the experimental data of fig. 1. Dotted line: linear spin-wave result for  $T=0$  fitted to the experimental two-magnon absorption for  $J_{12}/J=0.58$  and a two-magnon decay rate of  $0.09E_{op}$ . Inset: peak positions of the lower ( $E_{2a}$ ) and upper ( $E_{2b}$ ) two-magnon resonances in units of  $E_{op}$  for negligible broadening. Arrows indicate the experimental values.

in the inset of fig. 3. With  $E_{op} = 178$  meV we obtain  $J \approx 117$  meV and  $J_{12} \approx 68$  meV <sup>(5)</sup>. We point out that the two-magnon spectrum is not necessary to determine  $J$  and  $J_{12}$ . It is sufficient to know the slope of the acoustic magnon branch from neutron scattering and the position of the one-magnon peak to deduce the value of  $J_{12}$ : with  $J = (120 \pm 20)$  meV [6] we find  $J_{12} = (68 \pm 11)$  meV. In this flow of logic the knowledge of the position of the  $E_{2a}$ -peak is not necessary to fix the coupling parameters but it rather confirms the interpretation that the peak is to be identified with the two-magnon resonance.

The shape of the two-magnon absorption in monolayers [12] seems to be quite similar, and the question arises if the interpretation of Lorenzana and Sawatzky [13] also holds for the bilayered  $\text{YBa}_2\text{Cu}_3\text{O}_6$ . It turns out that the  $E_{2a}$ -peak may not be explained as a phonon-assisted bimagnon absorption (PBM) process because the energy of this resonance is too low for a bimagnon plus the appropriate phonon (for any value of  $J_{12}$ ). We expect an energy of roughly 470 meV for this process (for  $J_{12}/J \simeq 0.5$ ). So the PBM might well account for part of the  $E_{2b}$ -resonance.

In conclusion, we presented the low-conductivity mid-infrared spectrum of  $\text{YBa}_2\text{Cu}_3\text{O}_{6.0}$  which is dominated by absorption due to magnons. Linear spin-wave theory is consistent with the measured spectrum, *i.e.* it explains the resonances at  $E_{op}$ ,  $E_{2a}$  and  $E_{2b}$  if a sizable bilayer coupling is assumed.

\*\*\*

We are indebted to P. WÖLFLE for many helpful discussions and his encouragement, and we also acknowledge useful discussions with A. ROSCH and G. A. SAWATZKY. This work

<sup>(5)</sup> Such a large value of  $J_{12}$  is not entirely unexpected, see the estimate of Barriquand *et al.* [21].

was supported by the Commission of the EC under contract no. CI 1-0526-M(CD) and by the High- $T_c$  program of Baden-Württemberg. It was supported in part by the DFG (MG, HPG) and by SFB 195 (TK).

## REFERENCES

- [1] Recent reviews on this topic are: KAMPF A. P., *Phys. Rep.*, **249** (1994) 219; BRENIG W., *Phys. Rep.*, **251** (1995) 153.
- [2] MILLIS A. J. and MONIEN H., *Phys. Rev. Lett.*, **70** (1993) 2810; *Phys. Rev. Lett.*, **71** (1993) 210(E); *Phys. Rev. B*, **50** (1994) 16606.
- [3] ALTSHULER B. L. and IOFFE L. B., *Solid State Commun.*, **82** (1992) 253.
- [4] UBBENS M. U. and LEE P. A., *Phys. Rev. B*, **50** (1994) 438.
- [5] SANDVIK A. W. and SCALAPINO D. J., *Phys. Rev. Lett.*, **72** (1994) 2777.
- [6] SHAMOTO S., SATO M., TRANQUADA J. M., STERNLIEB B. J. and SHIRANE G., *Phys. Rev. B*, **48** (1993) 13817.
- [7] ROSSAT-MIGNOD J., REGNAULT L. P., JURGUENS J. M., BURLET P., HENRY J. Y. and LAPERTOT G., in *Dynamics of Magnetic Fluctuations in High-Temperature Superconductors*, edited by G. REITER, P. HORSCH and G. C. PSALTAKIS (Plenum Press, New York, N.Y.) 1989.
- [8] VETTIER C., BURLET P., HENRY J. Y., JURGENS M. J., LAPERTOT G., REGNAULT L. P. and ROSSAT-MIGNOD J., *Phys. Scr.*, **T29** (1989) 110.
- [9] LYONS K. B., FLEURY P. A., SCHNEEMEYER L. F. and WASZCZAK J. V., *Phys. Rev. Lett.*, **60** (1988) 732.
- [10] SUGAI S. *et al.*, *Phys. Rev. B*, **42** (1990) 1045.
- [11] GRÜNINGER M., ZIBOLD A., MÜNZEL J., GAYMANN A., GESERICH H. P. and KOPP T., to be published.
- [12] PERKINS J. D., GRAYBEAL J. M., KASTNER M. A., BIRGENEAU R. J., FALCK J. P. and GREVEN M., *Phys. Rev. Lett.*, **71** (1993) 1621.
- [13] LORENZANA J. and SAWATZKY G. A., *Phys. Rev. Lett.*, **74** (1995) 1867.
- [14] RENKER B., GOMPF F., GERING E., ROTH G., REICHARDT W., EWERT D., RIETSCHEL H. and MUTKA H., *Z. Phys. B*, **71** (1988) 437.
- [15] CHAKRAVARTY S., HALPERIN B. I. and NELSON D. R., *Phys. Rev. B*, **39** (1989) 2344.
- [16] MANOUSAKIS E., *Rev. Mod. Phys.*, **63** (1991) 1.
- [17] BONESTEEL N. E., *Phys. Rev. B*, **47** (1993) 11302.
- [18] MORIYA T., *J. Appl. Phys.*, **39** (1968) 1042, and references therein.
- [19] TRANQUADA J. M., SHIRANE G., KEIMER B., SHAMOTO S. and SATO M., *Phys. Rev. B*, **40** (1989) 4503.
- [20] ELLIOTT R. J. and THORPE M. F., *J. Phys. C*, **2** (1969) 1630.
- [21] BARRIQUAND F. and SAWATZKY G. A., *Phys. Rev. B*, **50** (1994) 16649.